

## Assessment of Multi-leaf Collimator Positional Accuracy Using Radiochromic EBT3 Film and an Electronic Portal Imaging Device

Forough NIKEGHBALI

*Medical Physics Department, Faculty of Medicine,  
Shahid Sadoughi University of Medical Sciences, Yazd 8915173149, Iran*

Abolfazl NICKFARJAM\*

*Medical Physics Department, Faculty of Medicine,  
Shahid Sadoughi University of Medical Sciences, Yazd 8915173149, Iran and  
Radiotherapy Research Center, Shahid Sadoughi University of Medical Sciences, Yazd 8915173149, Iran*

Fateme SHIRANI and Nouraddin Abdi GOUSHBOLAGH

*Medical Physics Department, Faculty of Medicine,  
Shahid Sadoughi University of Medical Sciences, Yazd 8915173149, Iran*

Nasim NAMIRANIAN

*Yazd Diabetes Research Center, Shahid Sadoughi University of Medical Sciences, Yazd 8915173149, Iran*

Bagher FARHOOD

*Department of Medical Physics and Radiology, Faculty of Paramedical Sciences,  
Kashan University of Medical Sciences, Kashan 8731753153, Iran*

Masoud SHABANI and Kazem VAKILI

*Radiotherapy Research Center, Shahid Sadoughi University of Medical Sciences, Yazd 8915173149, Iran*

(Received 1 July 2019; revised 7 November 2019; accepted 28 November 2019)

This study aimed to evaluate multi-leaf collimator (MLC) positional accuracy by using an electronic portal imaging device (EPID) and radiochromic EBT3 film. Furthermore, the MLC's positional accuracy at different gantry and collimator angles of a Siemens ONCOR linear accelerator (linac) was evaluated. A picket fence test was performed to evaluate the MLC's positional accuracy at various gantry and collimator angles of the linac. The EPID and the EBT3 films were sequentially irradiated seven times at 2-cm intervals by making a rectangular field ( $0.3 \times 19 \text{ cm}^2$ ). The full-width at half-maximum (FWHM) of each band (field) was calculated for all leaves by using inhouse software. Then, variations between the actual and the planned leaf locations were obtained by using the EPID and the EBT3 film at various gantry and collimator angles. The mean FWHM, acquired using the EPID and the EBT3 film ranged from 2.331 – 3.647 mm and 2.059 – 4.001 mm, respectively. Variations between the actual and the planned leaf locations were found to be affected by changes in the collimator and the gantry angles. Moreover, a  $-0.060 - 1.588$  mm difference we seen between the result obtained from the EBT3 film and that obtained from the EPID. The mean FWHM, at most angles, for the EBT3 film was larger than that for the EPID. The findings showed average deviations for the EPID (0.001 – 0.669 mm) and EBT3 film (0.007 – 1.001 mm); these values agreed within the tolerance level ( $\pm 1$  mm). Furthermore, good agreement was found between the results obtained from the EPID and the EBT3 film; these two dosimetric methods can be used interchangeably, but each must be chosen considering its advantages and disadvantages.

PACS numbers: 06.20.Dk, 06.20.F–, 06.20.fb

Keywords: Quality assurance, MLC, EPID, EBT3, Picket fence test

DOI: 10.3938/jkps.76.795

---

\*E-mail: nickfarjam6262@gmail.com

## I. INTRODUCTION

Radiotherapy (RT) is one of the main modalities in cancer treatment. As a multimodality treatment composed of surgery and/or chemotherapy, it plays a significant role in curing patients with cancer [1,2]. Over the past 20 years, RT has been enhanced from two-dimensional (2D) therapy to three-dimensional conformal treatment (3D-CRT) aimed at delivering more accurate radiation to target volumes while sparing surrounding normal tissue [3]. In addition, intensity-modulated radiation therapy (IMRT) is one of the most important technical advances in RT [4].

In these advanced radiotherapeutic techniques, the isodose surfaces with high and low values are conformed to the tumor surface and to critical organs adjacent to the tumor, respectively [5]. In this regard, multileaf collimators (MLCs) are used to conform the treatment field as close as possible to the target volume (for instance in 3D-CRT and IMRT) and/or to modulate the beam intensity (for instance in IMRT) [6,7]. Other applications of MLCs are to replace conventional blocking, increase the probability of local tumor control, automate radiation field setup and improve treatment efficacy [8].

If the correct dose is to be delivered to target volume, must be accurately and precisely controlled. The speed, acceleration, and position of MLCs, as planned by the treatment planning system (TPS) [6]. Several ways, such as using radiochromic and radiographic film, ionization chamber/diode arrays and electronic portal imaging devices (EPID), are used to control the MLCs. Ionization chambers and diodes, as point dosimeters, can only be used for positioning verification of a single leaf and are limited in spatial resolution; therefore, they are not appropriate for measurements with high spatial resolution. Radiographic films are another option, but their energy dependence, sensitivity to light, and processing reduce the application of these films for accurate work. Within the last 10 years, radiochromic EBT/EBT2/EBT3 films have acquired widespread use in radiation dosimetry [9, 10]. Sub-mm spatial resolution, relative energy dependence over a wide range of beam qualities used for RT, nearly water-equivalency, less sensitivity to room light and self-development make them suitable for dose measurement and quality assurance (QA) in RT [11]. Moreover, the EPID was developed as a tool to determine the accuracy of MLC positioning and has been shown to be suitable for this purpose because of desirable characteristics such as fast image acquisition, digital format, high resolution, potential for in vivo dosimetry, and 3D dose verification [9,12–14].

As mentioned above, the QA of MLC has a significant role in treatment planning and dose delivery, and differences between the planned and the actual leaf positions can lead to inaccurate dose distributions [15]. If an actual clinical advantage is to be gained from treatment, MLC technology must perform accurately according to

the treatment planning parameters [16]. The tools used for MLC positioning are primarily based on EPID and film methods [17,18]. Hence, the present study aimed to assess MLC positional accuracies obtained using the EPID and radiochromic EBT3 film; based on our knowledge, this is the first time that EBT3 film is used for this purpose in a step-and-shoot IMRT technique. The results for the film were compared with those obtained from the EPID. Furthermore, the MLC's positional accuracy at different gantry and collimator angles of a Siemens ONCOR linear accelerator (linac) was evaluated.

## II. MATERIALS AND METHODS

### 1. Radiation Unit, MLC and EPID

The exposures were done with a Siemens ONCOR Impression plus linac (Siemens Medical Systems, Concord, CA, USA). This system utilizes an MLC designed with double-focused and 41 pairs of leaves with a thickness of 75 mm. Each of the 39 inner leaves back project to a 10-mm width at 100 cm from the source while the 2 outer leaves back project to 5 mm in the isocenter plane (leaves #1 and #41). The leaves can travel across the beam's central axis for a maximum distance of 100 mm.

A Siemens OptiVue 500 EPID (Siemens Medical Systems, Concord, CA, USA) was used as the portal imager; its amorphous silicon (amsi) plate size is  $40 \times 40 \text{ cm}^2$  with a resolution of  $512 \times 512$  pixels and a pixel size of 0.8 mm. A 3-mm copper plate covers the sensitive layer of the EPID to eliminate low energy photons, followed by a scintillating layer of phosphor to convert incoming ionizing radiation (X-rays) to detectable light; then, a pixel array is implanted on the amorphous silicon panel to capture visible light and convert it to electric charge. The charge signals are then read out and digitized by using a 16-bit analogue-to-digital converter (ADC). The EPID is mounted at a source-to-surface distance (SSD) between 115 cm and 160 cm.

### 2. Picket Fence Test

In the picket fence test, the MLC leaf pairs sweep across the field, irradiating a slit field of 3 mm in width and 19 cm in height at intervals of 2 cm continuously 7 times. This irradiation protocol was delivered to the EPID and the radiochromic EBT3 film at fixed positions, which detects the MLC leaf position errors and allows the distance between opposing leaves to be evaluated [15,17, 19,20]. These procedures were done at four gantry and collimator angles of 0, 90, 180 and 270°.

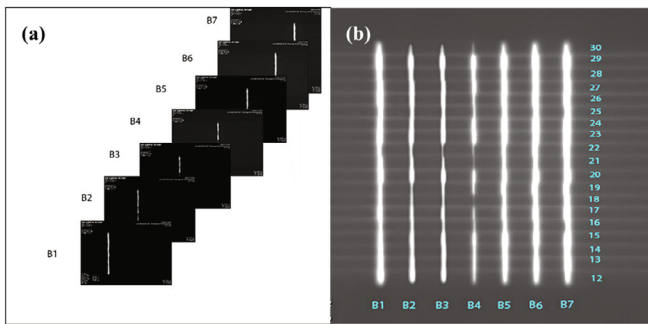


Fig. 1. (a) Portal images and (b) composite image for the picket fence test. That the slit fields of white and black demonstrate irradiated and unirradiated regions, respectively, is notable.

### 3. The Picket Fence Test as applied on the EPID

All portal images were taken using a 6-MV photon beam at a source-to-imager distance (SID) of 140 cm with 1 monitor unit (MU) per field [21]. The images with  $512 \times 512$  pixels were exported from the EPID acquisition software, and the pixel dimensions were approximately  $0.57 \times 0.57 \text{ mm}^2$  at the isocenter (100 cm). A composite image was created as a sum of the seven images by using in-house software (Figure 1).

### 4. The Picket Fence Test with the EBT3 film

The EBT3 films were placed on the treatment table at the isocenter level and exposed with 300 MUs per field (a total of 2100 MUs) at a SID of 100 cm without any additional buildup to create a sharper image. The films were scanned using a flatbed Microtek ScanMaker 9800XL Plus scanner (Microtek International, Inc. MRS3200A3L, China) 24 hours after irradiation. This allow for maximum post irradiation coloration. All exposed films were located with a scan ruler in the center of the scanner and was scanned in three colors (48-bit RGB) with a 75-dpi scanning resolution in the transmission mode with all image corrections switched off. Then, a Gaussian blur filter was applied to obtain smooth profiles. The films were scanned using Microtek Scan Wizard Pro software (Microtek Inc., China) four times, but only the last scan was kept for analysis and saved in a tagged image file format (.tiff files) for analysis (Figure 2) [18].

### 5. Image Analysis

Although the visual inspection was basically performed using picket fence tests with and without MLC

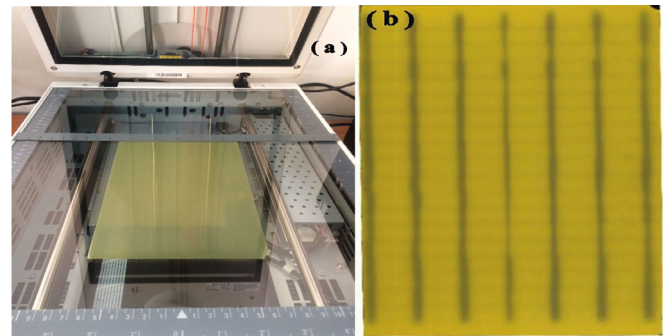


Fig. 2. (a) Scanning the irradiated EBT3 film and (b) the film image after scanning. The picket fence test shows seven pickets (stripes).

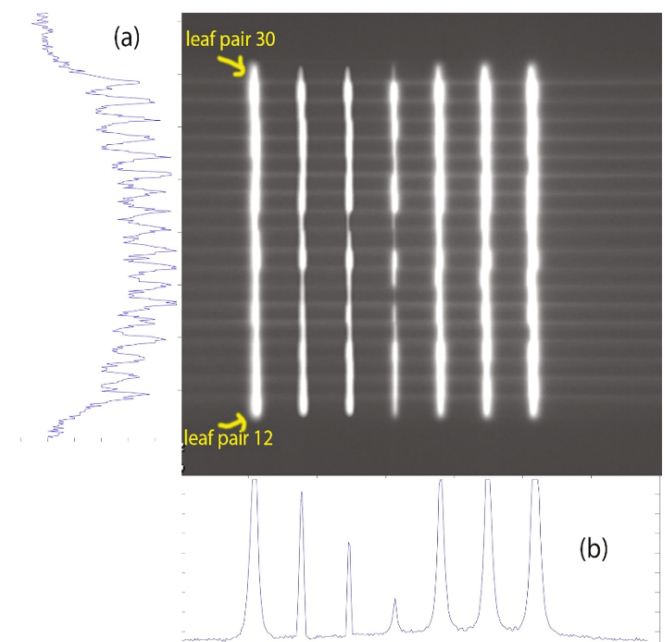


Fig. 3. (a) Portal images intensity profile perpendicular to the movement of the leaves to find the center of the MLCs and (b) intensity profile across the pickets at the position of the central leaf.

leaf position errors, in this study, with a further analysis, the radiation width and its deviation from the nominal width or MLC leaf position error were measured. MLC leaf position error is defined as the distance between the calculated position and the nominal planned position. For further processing, the portal images and raw images of the irradiated film were imported to in-house software, MATLAB R2008a (Math Works Inc, Natick, MA, USA). Then, the intensity profiles perpendicular to the movement of the leaves were plotted to find the center of the MLCs by identifying the position of the minimum points (valley) of the intensity profile in portal images and the maximum points (peak) of the intensity profile acquired using the EBT3 film (Figure 3(a)). The intensity profiles along the total pathway of the leaves were extracted

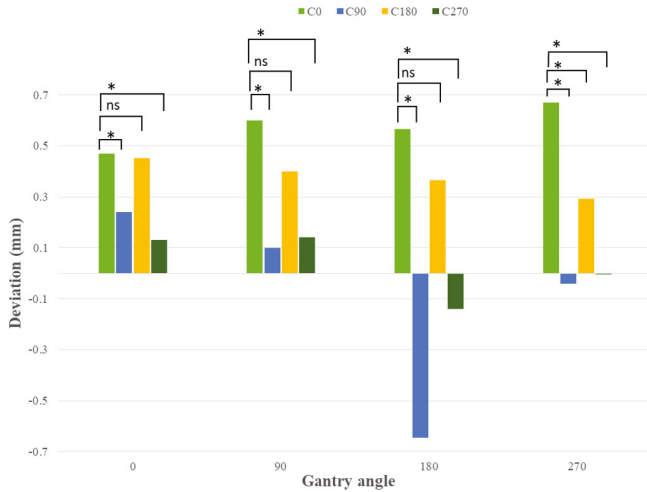


Fig. 4. Deviations from planned position for the EPID at four collimator gantry and angles. The groups labeled with \* have  $P < 0.05$  and “ns” means not significant.

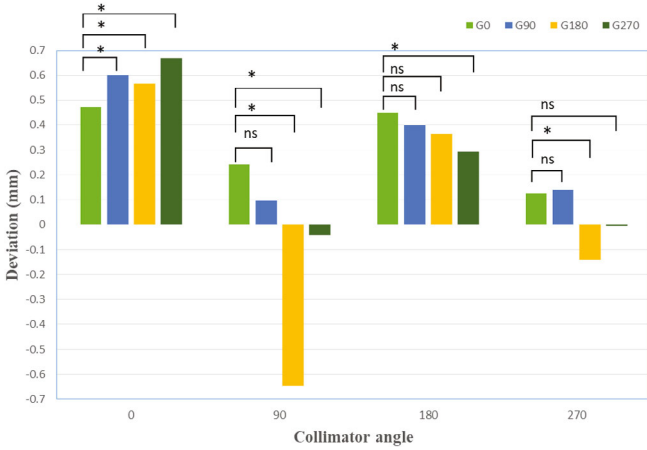


Fig. 5. Results from the EPID for evaluating the effect of gantry rotation on radiation width (FWHM) at four collimator and gantry angles. The groups labeled with \* have  $P < 0.05$  and “ns” means not significant.

at the position obtained in the previous step for each MLC (Figure 3(b)). The radiation gap width for each field was evaluated using the full width at half maximum (FWHM) of the narrow peaks, which correspond to the irradiated bands. It can then be compared to the nominal gap width, which was chosen to be 3 mm. That the tolerance level is  $\pm 1$  mm in IMRT is noteworthy [22].

### III. RESULTS

#### 1. Picket Fence Test Results for the EPID

The means and the standard deviations of the FWHM acquired using the EPID for all the leaf pairs at gantry angles of  $0^\circ$  and  $90^\circ$  and collimator angles of  $0, 90, 180$

Table 1. Results from the EPID to calculate the radiation width (FWHM). The FWHM is measured in millimeters.

Gantry (G) and Collimator (C) angle	Mean FWHM (mm)	Std. Error Mean FWHM
G0-C0	2.528	0.075
G0-C90	2.760	0.070
G0-C180	2.554	0.140
G0-C270	2.875	0.087
G90-C0	2.400	0.084
G90-C90	2.905	0.108
G90-C180	2.601	0.145
G90-C270	2.862	0.074
G180-C0	2.434	0.076
G180-C90	3.647	0.179
G180-C180	2.635	0.140
G180-C270	3.141	0.108
G270-C0	2.331	0.064
G270-C90	3.647	0.179
G270-C180	2.708	0.128
G270-C270	3.001	0.069

and  $270^\circ$  are tabulated in Table 1. The results in this table show the mean gap width when the center of the slit field ranged from  $-6.06$  cm to  $6.06$  cm in interval of 2 cm. The minimum deviation from the planned gap was 0.001 mm at a gantry and a collimator angle of  $270^\circ$ , and the maximum deviation was 0.669 mm at a gantry angle of  $270^\circ$  and a collimator angle of  $0^\circ$ , which was less than 1 mm [22]. The deviations from the planned MLC location for gantry angles  $0, 90, 180$  and  $270^\circ$  for every collimator angle on the picket fence test are illustrated in Fig. 4. As can be seen from this figure, Paired t-test comparisons between a collimator angle of  $0^\circ$  and the other collimator angles for four gantry angles showed significant differences in the deviations from the planned leaf positions with collimator rotation ( $P < 0.003$ ), except for the G0-C180 ( $P = 0.869$ ), G90-C180 ( $P = 0.226$ ) and G180-C180 ( $P = 0.197$ ). The results of gantry rotation are shown in Fig. 5. Paired t-test comparisons between a gantry angle of  $0^\circ$  and the other gantry angles for four collimator angles showed significant differences in the mean radiation gap from the planned leaf positions with gantry rotation ( $P < 0.05$ ), except for the G90-C90 ( $P = 0.121$ ), G90-C180 ( $P = 0.303$ ), G180-C180 ( $P = 0.066$ ), G90-C270 ( $P = 0.867$ ) and G270-C270 ( $P = 0.116$ ).

#### 2. Picket Fence Test Results for the EBT3 Film

Table 2 shows the means and the standards deviation of FWHM, acquired using the EBT3 film for all leaf pairs at gantry angles of  $0^\circ$  and  $90^\circ$  and collimator angles of

Table 2. Results from the EBT3 film to calculate the radiation width (FWHM). The FWHM is measured in millimeters.

Gantry (G) and Collimator (C) angle	Mean FWHM (mm)	Std. Error Mean FWHM
G0-C0	2.307	0.062
G0-C90	2.617	0.063
G0-C180	2.821	0.048
G0-C270	3.007	0.060
G90-C0	2.716	0.068
G90-C90	2.965	0.063
G90-C180	2.508	0.054
G90-C270	2.940	0.064
G180-C0	3.362	0.050
G180-C90	4.001	0.055
G180-180	3.292	0.048
G180-C270	3.905	0.055
G270-C0	2.059	0.040
G270-C90	2.818	0.053
G270-C180	2.508	0.054
G270-C270	2.977	0.056

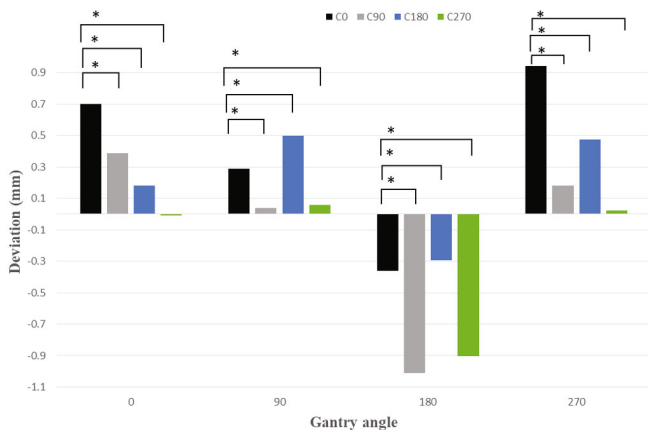


Fig. 6. Deviations from planned position for the film at four collimator and gantry angles. The groups labeled with \* have  $P < 0.05$ .

0, 90, 180 and 270°. The findings presented in this table show that the mean gap width when the center of the slit field ranged from  $-6.06$  cm to  $6.06$  cm in intervals of 2 cm. The minimum deviation from the planned gap was 0.007 mm at a gantry angle of 0° and a collimator angle of 270°, and the maximum deviation was 1.001 mm at a gantry angle of 180° and a collimator angle of 90°. Figure 6 shows the deviations from the planned MLC locations for four gantry and collimator angles on the picket fence test. Paired t-test comparisons between a collimator angle of 0° and the other collimator angles for gantry angles of 0, 90, 180 and 270° showed significant differences in deviations from the planned position with

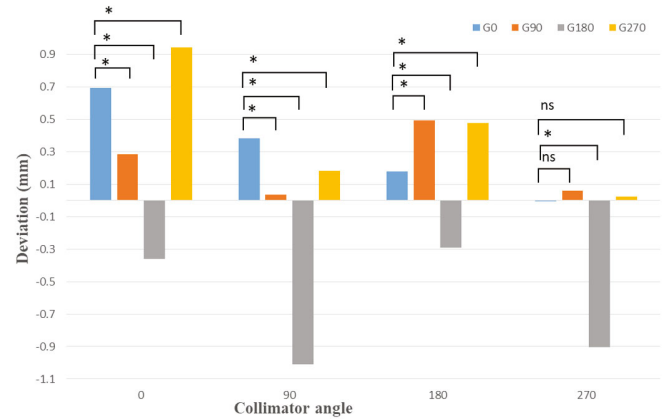


Fig. 7. Results from the film for evaluating the effect of gantry rotation on radiation width (FWHM) at four collimator and gantry angles. The groups labeled with \* have  $P < 0.05$  and “ns” means not significant.

the collimator rotation for all collimator angles ( $P < 0.05$ ).

The results obtained from the EBT3 film for gantry rotation are illustrated in Fig. 7. As can be seen from this figure, Paired t-test comparisons between a gantry angle of 0° and the other gantry angles for four collimator angles reveal significant differences in the radiation gap width ( $P < 0.05$ ), except the G90-C270 ( $P = 0.414$ ) and G270-C270 ( $P = 0.603$ ).

### 3. Comparison of the Results for the EBT3 Film and the EPID

The results obtained from assessments of the MLC’s positional accuracy by using the EBT3 film and by using the EPID are compared in Table 3. For most cases, the mean values of the radiation width for both the EBT3 film and the EPID were within the tolerance level,  $\pm 1$ mm. The difference range between the result obtained from the EBT3 film and from the EPID was  $-0.060$  –  $1.588$  mm.

## IV. DISCUSSION

In advanced radiotherapeutic techniques (such as 3D-CRT and IMRT), the QA of the MLC has a significant role in treatment planning and dose delivery, and for this reason, in the present study, the MLC’s positional accuracy at different gantry and collimator angle of the Siemens ONCOR linac was investigated by using a EPID and EBT3 film. The findings obtained using the EPID and EBT3 film (Figures 4 and 6) demonstrate that the variations between the actual and the planned leaf locations for four gantry angles and for every collimator angle on the picket fence test were less than 1 mm; hence, these

Table 3. Comparison of the results obtained from assessments of the MLC's positional accuracy by using the EBT3 film with those of the EPID at various gantry and collimator angles.

Gantry (G) and Collimator (C) angle	Mean FWHM of EPID	Mean FWHM of Film	Difference (mm)
G0-C0	2.528	2.307	0.221
G0-C90	2.760	2.617	0.143
G0-C180	2.554	2.821	-0.267
G0-C270	2.875	3.007	-0.132
G90-C0	2.400	2.716	-0.316
G90-C90	2.905	2.965	-0.060
G90-C180	2.601	2.508	0.093
G90-C270	2.862	2.940	-0.078
G180-C0	2.434	3.362	-0.928
G180-C90	3.647	4.001	-0.354
G180-C180	2.635	3.292	-0.657
G180-C270	3.141	3.905	-0.764
G270-C0	2.331	2.059	0.272
G270-C90	3.647	2.818	1.588
G270-C180	2.708	2.508	0.200
G270-C270	3.006	2.977	0.029

values agreed with the tolerance level for leaf positions of an IMRT field advocated by the American Association of Physicists in Medicine (AAPM) Task Group No. 142 ( $\pm 1$  mm) [22]. In a study by Antypas *et al.* [18], MLC positional accuracy through the picket fence test for the EBT2 films and a 3D volumetric phantom was examined. In that study, the FWHMs of the narrow peaks, which corresponded to the irradiated bands, were calculated, and the actual gap width was found to range between 0.25 and 0.29 cm, instead of the nominal 0.3 cm, which is considered to be within safe limits. These results are similar to our results for the EPID, 0.23 – 0.36 cm, and of the EBT3 film, 0.21 – 0.40 cm. LoSasso *et al.* evaluated the physical and dosimetric aspects of MLCs and reported a MLC precision of 0.25 mm [23], which is close to our findings in terms of the average deviation.

Regarding the impact of the collimator rotation on the radiation width (Figures 5 and 7), we found a significant difference between most angles of the collimator in comparison with the angle of  $0^\circ$ , but those differences were within the tolerance level ( $\pm 1$  mm) [22]. Evaluating the effect of the gantry rotation also showed a significant difference between all gantry angles in comparison with the gantry angle of  $0^\circ$ , but those differences were again within the tolerance level ( $\pm 1$  mm) [22]. In a study by Sumida *et al.*, leaf position was verified by using an EPID, and their results showed a significant difference in the deviations from the planned leaf position at four

gantry angles. They suspected this difference to be due to the narrowing orientation of the leaf along the central axis [15]. Those results were close to our findings. Ling *et al.* [24] evaluated the accuracy of dynamic multileaf collimators (DMLC) position during gantry rotation by using the picket fence test and reported that the effect of gantry rotation on leaf accuracy was  $\leq 0.2$  mm. These data agree with our finding. One of our reasons for variations between the actual and the planned leaf locations for different gantry angles is that these differences arise from the effect of gravity on the leaf's position, but the results of Parent *et al.* study [25] at gantry angles of  $90^\circ$  and  $270^\circ$  showed no significant effect of gravity on leaf positions. Moreover, Antypas *et al.* [18] showed that gravity does not significantly affect the MLC performance.

Our other results (Table 3) demonstrated that the mean FWHM, at most angles, for the EBT3 film is larger than that for the EPID. Nevertheless, at most angles, a good agreement was seen between the results obtained using the EPID and the EBT3 film. In a study, Li *et al.* [16] evaluated the MLC leaf position and speed based on a EPID and EBT3 film for dynamic IMRT treatment. They reported that the difference between the EPID and the film results for the MLC position was less than 0.1 mm; thus, these results showed an agreement between two methods. The reported value in their study was less than our findings ( $-0.060 - 1.588$  mm). In the comparison between the EPID and the EBT3 film, another concern is that the effective pixel size of the EPID is 0.57 mm when projected back to the isocentric plane while the EBT3 film's pixel size is 0.33 mm, which is smaller than the EPID's. Chang *et al.* [21] showed that the dose profiles of the DMLC test pattern using scanning pixel sizes of 0.75 mm overlap very well with these using 0.37 mm pixel size. As reported by other studies [16,21,26,27], these two dosimetric methods (EPID and EBT3 film) interchangeably, but each must be chosen considering its advantages and disadvantages. For example, the film is an analog tool, so digitizing is a time-consuming process and requires significant manpower, making it very tedious for routine use in QA, but the EPID is a faster and more effective tool for QA. However, the spatial resolution of the film is better than that of the EPID.

In the current study, the MLC's positional accuracy only between leaf pairs 12 to 30 was analyzed, and the other MLC positional accuracies were not analyzed. However, the several studies [15,16,18], which have been evaluated the MLC positional accuracy by using the 'picket fence test' and the irradiated field size used in these studies, were similar to our study in that not all MLC errors were analyzed because the film's dimensions were insufficient to cover all MLCs in the isocenter.

## V. CONCLUSION

In the current study, the MLC's positional accuracy of a Siemens ONCOR linac was investigated by using a EPID and EBT3 film. The results showed slight leaf deviation for the EPID (0.001 – 0.669 mm) and EBT3 film (0.007 – 1.001 mm); these values agreed within the tolerance level ( $\pm 1$  mm). Furthermore, variations between the actual and the planned leaf locations were found to be affected by variations in the collimator and the gantry angles. Also, good agreement was seen between the results obtained from the EPID and the EBT3 film; thus, these two methods can be used interchangeably, but each must be chosen considering its advantages and disadvantages.

## ACKNOWLEDGMENTS

This article was extracted from a M. Sc. thesis in medical physics by the first author and it was supported by Shahid Sadoughi University of Medical Sciences, Yazd, Iran (IR.SSU.MEDICINE.REC.1396.157). The measurements data were carried out at Shahid Ramezan Zadeh Radiotherapy Center, Yazd, Iran. Therefore, the authors express their sincere appreciation to the above center for its support.

## REFERENCES

- [1] N. Abdi Goushbolagh *et al.*, *Artif. Cells Nanomed. Biotechnol.* **46**, S1215 (2018).
- [2] N. A. Goushbolagh *et al.*, *Bionanoscience* **8**, 769 (2018).
- [3] N. Lee and S. Terezakis, *J. Surg. Oncol.* **97**, 691 (2008).
- [4] G. A. Ezzell *et al.*, *Med. Phys.* **30**, 2089 (2003).
- [5] K. Jabbari, A. Amouheidari and S. Babazadeh, *Int. J. Mol. Sci.* **9**, 111 (2012).
- [6] F. M. Khan and J. P. Gibbons, *Khan's the Physics of Radiation Therapy* (Wolters Kluwer, Philadelphia, 2014), Chap. 19, pp. 413–430.
- [7] C. S. Hong *et al.*, *Med. Phys.* **41**, 2 (2014).
- [8] A. R. T. Committee and A. Boyer, *AAPM Report No.* 72, 2001.
- [9] M. Mohammadi and E. Bezak, *Phys. Med. Biol.* **52**, N21 (2006).
- [10] G. Sim, J. Wong and K. Ng, *J. Appl. Clin. Med. Phys.* **14**, 85 (2013).
- [11] S. Devic, *Phys. Medica* **27**, 122 (2011).
- [12] W. van Elmpt *et al.*, *Radiother. Oncol.* **88**, 289 (2008).
- [13] G. J. Budgell and M. F. Clarke, *Phys. Med. Biol.* **53**, N297 (2008).
- [14] S. J. K. Baker, G. J. Budgell and R. I. MacKay, *Phys. Med. Biol.* **50**, 1377 (2005).
- [15] I. Sumida *et al.*, *J. Radiat. Res.* **53**, 798 (2012).
- [16] Y. Li *et al.*, *J. Appl. Clin. Med. Phys.* **18**, 106 (2017).
- [17] A. Agnew *et al.*, *Phys. Med. Biol.* **59**, N49 (2014).
- [18] C. Antypas *et al.*, *J. Appl. Clin. Med. Phys.* **16**, 189 (2015).
- [19] M. Mamalui-Hunter, H. Li and D. A. Low, *Med. Phys.* **35**, 2347 (2008).
- [20] C. S. Chui, S. Spirou, and T. LoSasso, *Med. Phys.* **23**, 635 (1996).
- [21] J. Chang *et al.*, *Med. Phys.* **31**, 2091 (2004).
- [22] E. E. Klein *et al.*, *Med. Phys.* **36**, 4197 (2009).
- [23] T. LoSasso, C. S. Chui and C. C. Ling, *Med. Phys.* **25**, 1919 (1998).
- [24] C. C. Ling *et al.*, *Int. J. Radiat. Oncol. Biol. Phys.* **72**, 575 (2008).
- [25] L. Parent *et al.*, *Med. Phys.* **33**, 3174 (2006).
- [26] M. Wendling *et al.*, *Med. Phys.* **33**, 259 (2006).
- [27] C. Agnew, P. Jeevanandam, P. Sukumar and M. Grat-tan, *Biomed. Phys. Eng. Express* **4**, 025017 (2018).